BIOCHEMISTRY
including biophysical chemistry & molecular biology

Article

pubs.acs.org/biochemistry

Heme Stabilization of α-Synuclein Oligomers during Amyloid Fibril Formation

Eric Y. Hayden,[*,†,∥] Prerna Kaur,[‡] Thomas L. Williams,[§] Hiroshi Matsui,[‡] Syun-Ru Yeh,[†] and Denis L. Rousseau[*,†]

[†]Department of Physiology and Biophysics, Albert Einstein College of Medicine of Yeshiva University, Bronx, New York 10461, United States

[‡]Department of Chemistry, Hunter College and Graduate Center, The City University of New York, New York, New York 10021, United States

[§]Department of Physiology and Biophysics, Case Western Reserve University, Cleveland, Ohio 44106, United States

Supporting Information

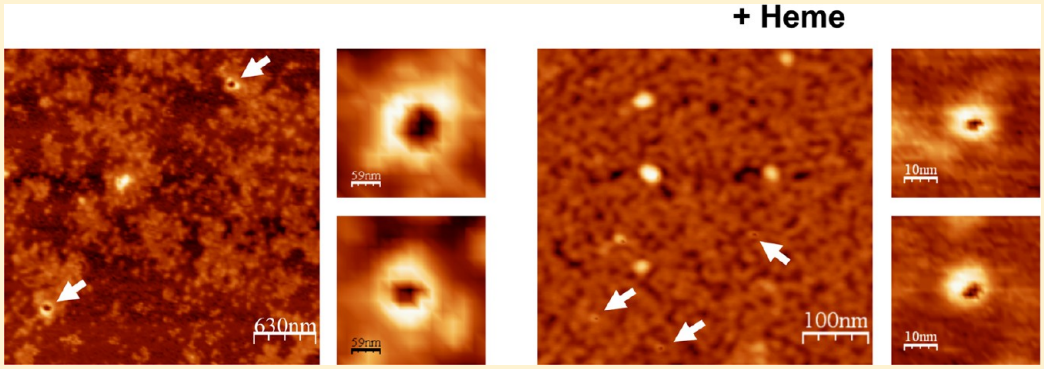

ABSTRACT: α-Synuclein (αSyn), which forms amyloid fibrils, is linked to the neuronal pathology of Parkinson's disease, as it is the major fibrillar component of Lewy bodies, the inclusions that are characteristic of the disease. Oligomeric structures, common to many neurodegenerative disease-related proteins, may in fact be the primary toxic species, while the amyloid fibrils exist either as a less toxic dead-end species or even as a beneficial mechanism for clearing damaged proteins. To alter the progression of the aggregation and gain insights into the prefibrillar structures, we determined the effect of heme on αSyn oligomerization by several different techniques, including native (nondenaturing) polyacrylamide gel electrophoresis, thioflavin T fluorescence, transmission electron microscopy, atomic force microscopy, circular dichroism, and membrane permeation using a calcein release assay. During aggregation, heme is able to bind the αSyn in a specific fashion, stabilizing distinct oligomeric conformations and promoting the formation of αSyn into annular structures, thereby delaying and/or inhibiting the fibrillation process. These results indicate that heme may play a regulatory role in the progression of Parkinson's disease; in addition, they provide insights into how the aggregation process may be altered, which may be applicable to the understanding of many neurodegenerative diseases.

In neurodegenerative diseases, including Alzheimer's disease (AD), Parkinson's disease (PD), and prion diseases, proteinaceous deposits, comprised of fibrils with a common β-sheet amyloid structure, have been found in the brain.[1] These deposits result from misfolding of the disease-related protein, which undergoes a conformational change from its initial structure to a cross-β sheet amyloid fold.[2] In patients with PD, and to a lesser extent AD, the deposits contain aggregates of the protein α-synuclein (αSyn).[3] Conformational changes of αSyn from random coil to a β-pleated sheet structure lead to the formation of insoluble αSyn fibrils that are the building blocks of the pathological inclusions.[4,5]

Recent evidence implicates prefibrillar structures common to many disease-related proteins as the most toxic forms of these proteins, supporting the notion that the insoluble amyloid deposits may be either a less toxic dead-end species or a beneficial storage mechanism for quarantining damaged proteins.[6−11] It has been observed that a collection of amyloid-forming proteins, including αSyn, can undergo a supramolecular assembly, and in reconstituted membranes, they can form morphologically comparable ion-channel-like structures that elicit ion-channel currents.[11] It is plausible that these ion channels could destabilize cellular ionic homeostasis and thus be the common structure of these proteins that induces cell pathophysiology and degeneration in amyloid diseases. Further, the link between αSyn fibrillization and PD neuro-

Received: March 13, 2015
Revised: July 10, 2015
Published: July 10, 2015

DOI: 10.1021/acs.biochem.5b00280
Biochemistry 2015, 54, 4599−4610

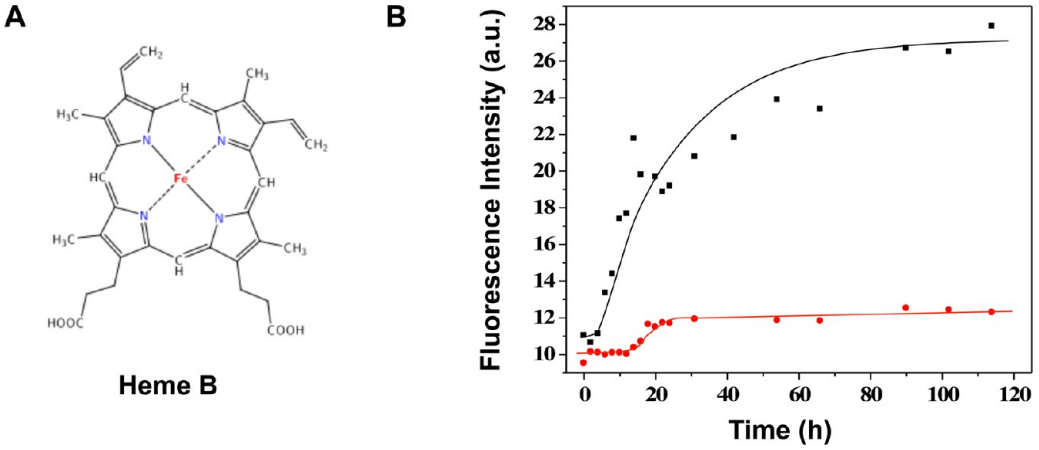

Figure 1. (A) Molecular structure of heme B. (B) Time course of thioflavin T (ThT) fluorescence, excited at 446 nm, in the absence and presence of heme with αSyn. αSyn (90 μM) was incubated at 37 °C while being shaken at 250 rpm over a period of 115 h in PBS (pH 7.4). In the absence of 90 μM heme, there is an increase in the fluorescence at 490 nm with an increasing incubation time, corresponding to the formation of amyloid structures. In the presence of heme, there is an extension of the lag phase, as well as an overall decrease in ThT fluorescence intensity.

toxicity may involve inappropriate membrane permeabilization by a prefibrillar species.[12,13] In aqueous solution, αSyn is a natively unstructured protein. Recent studies suggest that it may exist as a tetramer physiologically,[14,15] but these conclusions have been called into question.[16] Upon interaction with membranes or micelles, two regions of α-helical structure form, while the C-terminal region remains unstructured.[17−20]

It has been reported that interactions of heme (Figure 1A), and porphyrin, with αSyn may play a role in its pathophysiology and can be inhibitors of fibril formation with IC_{50} values in the low micromolar range.[21−23] Biochemical analysis revealed the formation of soluble oligomeric αSyn upon being incubated with heme, suggesting that this may be the mechanism by which filament formation is inhibited.[21] Unlike αSyn filaments and protofibrils, these soluble oligomeric species did not reduce the viability of SH-SY5Y cells. These findings suggest that the soluble oligomers formed in the presence of various inhibitory compounds may not be toxic to neuronal cells and that heme and related compounds may therefore have therapeutic potential for α-synucleinopathies and other brain amyloidoses. A study of the generic inhibitory properties of hemin on protein misfolding found that hemin could prevent fibril formation for κ-casein, amyloid β-protein, and αSyn but could not disaggregate preformed fibrils.[24] Lastly, it was found that heme did not inhibit filament formation of αSyn truncated by 20 amino acids (1−120), indicating that the C-terminal region is critical for the inhibitory interaction.[21]

In this work, we examined the structural and kinetic nature of the interaction of αSyn and heme (heme B) to determine the mechanisms by which heme alters oligomerization and aggregation. We found that interaction of heme with αSyn leads to the formation of unique low-molecular weight structures that could play a protective role in neurodegenerative disease.

EXPERIMENTAL PROCEDURES

Purification of αSyn. The cDNA of human αSyn (NACP140, clone IOH14008 from Invitrogen) was inserted into a glutathione *S*-transferase (GST) pGEX-4T-1 vector. The protein is expressed as a GST fusion protein and includes a thrombin cleavage site that allows for purification of human αSyn. This plasmid was transformed into *Escherichia coli* strain BL21(DE3). The protein was overexpressed by induction with isopropyl β-D-thiogalactopyranoside (IPTG) (Sigma) After induction with IPTG, the cells were incubated at 30 °C for 14−16 h before being sonicated in the presence of a protease inhibitor cocktail and centrifuged twice to remove cell debris. The remaining supernatant was subjected to ammonium sulfate precipitation up to 40%, over a 1 h period. After centrifugation, the resulting pellet was resuspended and centrifuged again to remove any small particles. The supernatant was then filtered and applied to a glutathione Sepharose column (GE Healthcare) at a flow rate of ≈0.2 mL/min. The bound fusion protein was then washed with 10 column volumes of sodium phosphate buffer (pH 7.6). αSyn was cleaved from the column-bound GST with thrombin overnight at 4 °C. This produced wild-type αSyn, except for the addition of Gly-Ser at the amino-terminal end, which remains from the thrombin cleavage site. The thrombin was removed from the mixture by directly connecting a benzamidine Sepharose column to the glutathione Sepharose column, which binds trypsin-like serine proteases. The purified αSyn was collected and then concentrated and immediately stored in liquid nitrogen.

It has been observed that ≈20% of the bacterially expressed human αSyn can be mistranslated in *E. coli* and that a cysteine residue is incorporated at position 136 instead of a tyrosine.[25] There are no native cysteine residues in αSyn, and it was observed that this misincorporation resulted in higher levels of dimeric αSyn because of disulfide bond formation. To avoid potential artifacts resulting from this misincorporation, using the Stratagene Quick-change site-directed mutagenesis kit we made this corrective mutation to the codon for tyrosine 136 from TAC to TAT. This mutation has been shown to result in reliable translation of tyrosine 136.[25] All αSyn purification is from the Y136-TAT construct, which is also termed αSyn. All experiments were conducted in phosphate-buffered saline (PBS), with 30 mM sodium phosphate and 150 mM NaCl (pH 7.6), unless otherwise specified.

Fibril Formation. Samples of 90 μM αSyn were incubated with or without 90 μM heme at 37 °C with 250 rpm shaking for 115 h. In one experiment, 0.02% NaN_3 was added to samples to ensure that there was no bacterial growth over the course of the experiment and was confirmed not to alter the results. Heme B (Frontier Scientific, Logan, UT) was prepared as a 1 mM stock

DOI: 10.1021/acs.biochem.5b00280
Biochemistry 2015, 54, 4599−4610

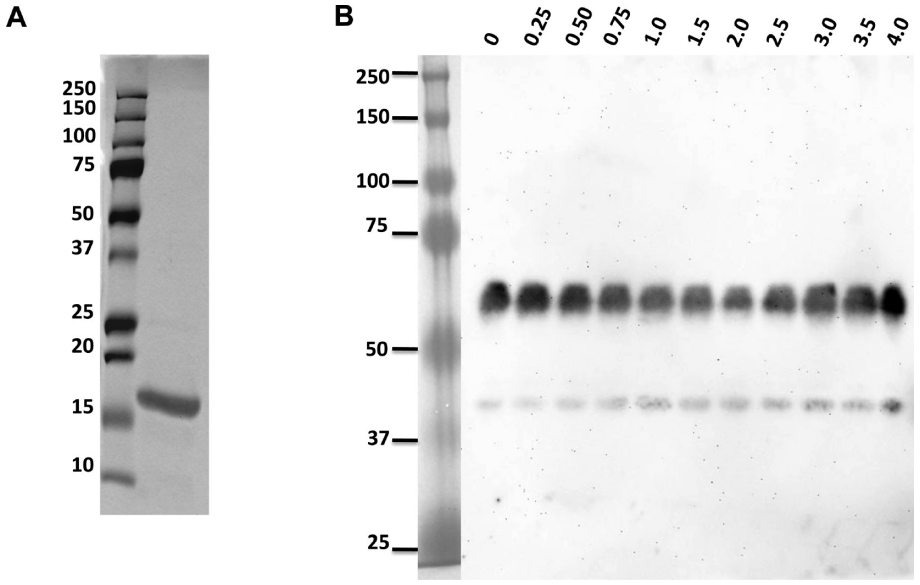

Figure 2. PAGE of αSyn. (A) SDS−PAGE of αSyn at time zero. The protein runs as a single band at ∼17 kDa. (B) Native PAGE of αSyn at time zero to 4 h. No change is observed in the size or oligomer distribution of αSyn.

in 10 mM NaOH and diluted in PBS (pH 7.6) to the appropriate concentration before each experiment. An equivalent amount (final concentration of 900 μM) of NaOH was added to the sample without heme to ensure identical conditions with and without heme. Aliquots were removed at various times and stored immediately in liquid nitrogen.

Thioflavin T Fluorescence. Immediately before measurement of the ThT spectrum, 7 μL of 90 μM αSyn was added to 1.793 mL of 50 mM Tris-HCl (pH 8.2), and finally, 200 μL of 100 μM ThT was added for a final volume of 2 mL. The final concentrations were 315 nM for αSyn and 10 μM for ThT. Spectra were acquired with an excitation of 446 nm (5 nm slits widths) from 460 to 700 nm at intervals of 1 nm with an integration time of 2 s. The fluorescence intensity of the emission spectrum was plotted at 490 nm.

Atomic Force Microscopy (AFM). AFM images were obtained with a Nanoscope IIIa (Digital Instruments, Santa Barbara, CA) in tapping mode on freshly cleaved mica substrates at a resonance frequency of ∼280 kHz. The scan rate was kept in the range of 0.8−2.0 Hz with 512 lines. A detailed structural analysis was performed using atomic force microscopy in noncontact "tapping" mode (AFM), and forces on the sample were limited to <2.8 N/m as dictated by the spring constant of the tip (PPP-FMR tips from Nanosensors). The typical tip radius is <7 nm. The samples for AFM investigation were identical to those described in Fibril Formation. One drop of sample was placed on a freshly cleaved mica surface, dried at room temperature, subsequently washed twice with water, and finally wicked off with filter paper. Analysis of structures was performed using WSxM software[26] by measuring the average height of the cross section of the structure of interest.

Transmission Electron Microscopy. Negative stain images were obtained with a JEOL 100CXII or 1200EX instrument at 80 kV. The samples for TEM investigation were identical to those described in Fibril Formation. Samples were adsorbed onto carbon/Formvar-coated 300 mesh copper grids after glow discharge and stained with 1% uranyl acetate.

Native Gel Polyacrylamide Gel Electrophoresis (PAGE) Western Blot. Samples were mixed with native sample buffer and loaded onto a 10% Tris-HCl polyacrylamide gel (Bio-Rad), run at 140 V followed by overnight transfer to a PVDF membrane at 40 V. The mouse monoclonal antibody against αSyn from Zymed Laboratories was used (Syn211) in conjunction with HRP-anti-mouse IgG (eBioscience) at a 1:1000 dilution for detection.

Circular Dichroism Measurements. αSyn was prepared as described above with a final protein concentration of 90 μM. Circular dichroism spectra were recorded on a JASCO J-815 CD spectrometer. Data were collected at room temperature in a 0.1 cm semimicro quartz cuvette (Hellma). Spectra were measured from 250 to 190 nm with a step size of 0.1 nm, a bandwidth of 1 nm, a response time of 4 s, and a scan speed of 20 nm/min. For all spectra, an average of two scans was obtained. CD spectra of the appropriate buffers were measured and found to contribute negligibly. Component analysis was conducted using CDPro based on CONTINLL and CONTIN3, from ref 27.

RESULTS

Heme Modifies Amyloid Fibril Formation of αSyn. Thioflavin T (ThT) was used to quantify the amyloid fibril formation of αSyn and to determine the impact of heme on the rate of fibril formation. αSyn was incubated with or without equimolar heme, 90 μM each, at 37 °C with agitation for 115 h. ThT fluorescence at 490 nm, as a function of incubation time, is plotted in Figure 1B. In the absence of heme, aggregation follows the expected nucleation-dependent fibril formation kinetics with a lag phase of 4 h followed by rapid growth of amyloid fibrils.[28] In the presence of heme, the duration of the lag phase increased to ∼15 h and the plateau level was reduced. The final intensity of the ThT fluorescence in the presence of heme is <10% of the intensity in the absence of heme. As reported by others, the ThT emission spectrum was not affected by the presence of heme (data not shown).[29]

Distinct αSyn Intermediates Are Identified by Native-PAGE in the Presence of Heme. To determine the

DOI: 10.1021/acs.biochem.5b00280
Biochemistry 2015, 54, 4599−4610

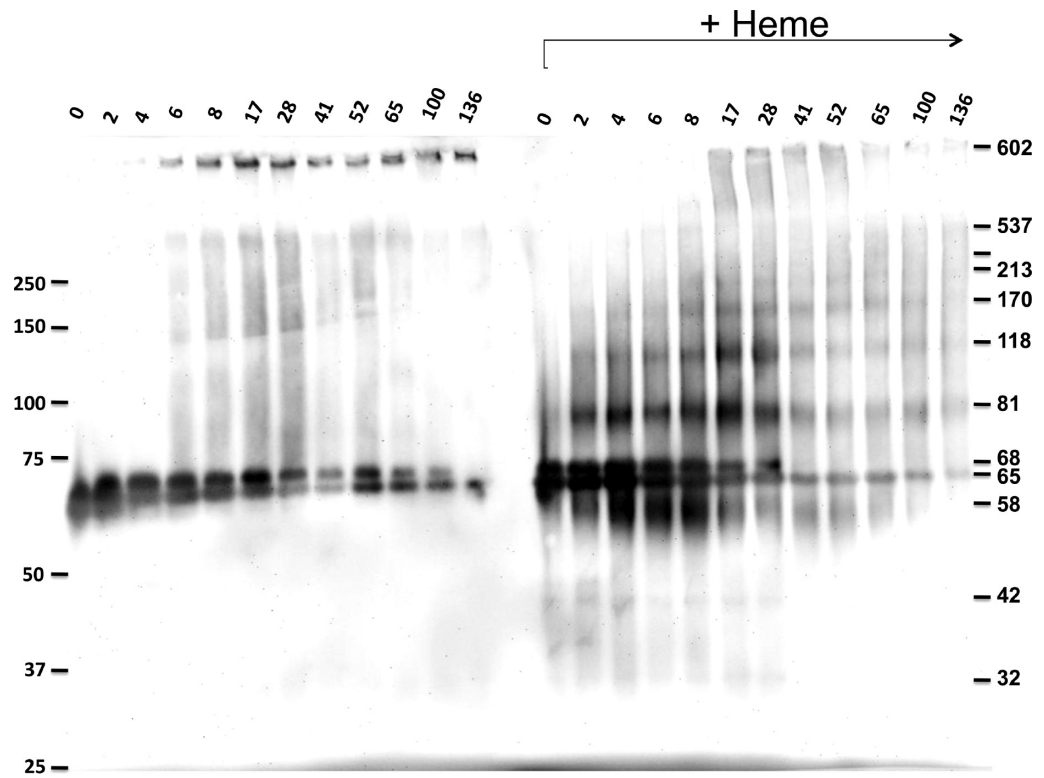

Figure 3. Native PAGE of αSyn upon incubation from 0 to 136 h in the absence and presence of heme. During the aggregation in the absence of heme, the initial species of αSyn forms protofibrillar and fibrillar structures after aggregation for 6 h as shown at the left. In contrast, in the presence of heme, a ladder of increasingly sized oligomeric structures is resolved on the gel. The results presented are representative of three different experiments. At the left is the position of marker proteins, while the right shows MWs calculated on the basis of the relative migration compared to the marker.

distribution of oligomer sizes formed during aggregation of αSyn, native (nondenaturing) polyacrylamide gel electrophoresis (native-PAGE) analyses were performed on samples with and without heme. αSyn was detected by Western blotting with antibody Syn211. We observed that Syn211 was able to detect αSyn in native, oligomeric, and fibril conformations. When αSyn (14 kDa) was examined by sodium dodecyl sulfate (SDS)−PAGE, we observe a single band that migrated to approximately 17 kDa (Figure 2A), as reported by others.[30]

In contrast to the SDS−PAGE analysis, native PAGE results showed that prior to incubation (t = 0) αSyn appears as a doublet, both with and without heme, displaying an apparent molecular weight of ∼60 kDa as shown in Figure 3. We propose that the doublet represents two related conformations[31] or two similar conformations that differ in their charge. It is also noteworthy that in the absence and presence of heme, the level of the higher-migrating species diminished faster than the lower component. When the protein is run via SDS−PAGE (Figure 2A), a doublet is not observed, suggesting that these species have the same molecular weight. The apparent molecular weight of ∼60 kDa is very interesting. Recent sedimentation equilibrium analytical ultracentrifugation (SE-AUC) and nuclear magnetic resonance (NMR) data both suggest that αSyn exists as a physiological tetramer of ∼57 kDa and directly correlate with a gentle purification scheme when produced recombinantly.[14,15] Our purification scheme indeed avoided boiling and denaturation; thus, the predominant band we observe at 60 kDa may be a stable tetramer. However, the assignment of an ∼60 kDa band as a tetramer has been called into question.[32] It has been reported that monomeric αSyn appears to be substantially larger when it is eluted from a gel-filtration column, equivalent to a molecular mass of 51 kDa.[33] More recently, Fauvet et al. pointed out that molecular weight estimations from native gels are unreliable.[32] They reported that αSyn from the brains of several species eluted at the same apparent molecular weight as the unfolded monomeric αSyn. On this basis, we refrain from assigning the 60 kDa band as a monomer or a tetramer and just label it as the "60 kDa" band.

At all times subsequent to the initial measurement, there are significant differences between αSyn incubated with or without heme as may be seen in Figure 3. The αSyn without heme displayed a band at the bottom of the sample well after incubation for 4 h. This is consistent with the 4 h lag phase that was determined by ThT fluorescence and thus may correspond to aggregated protein fibrils that are too large to enter the gel matrix. Concurrently, diffuse staining at the stacking and running gel interface is observed, indicating that specific oligomers are not preferentially formed. At aggregation times of >65 h, the intensity of the upper band of the initial species doublet appears to decrease earlier than that of the lower band, and finally, at 136 h the upper band of the two is no longer observed.

In contrast, in the presence of heme after 2 h, in addition to the initial 60 kDa band, a band at approximately 80 kDa appears, which we attribute to a stable oligomer of αSyn (Figure 3). At each increasing time point examined in the presence of heme, distinct bands of increasing size are populated, displaying a clear ladder of oligomers. On the basis of the MW marker, stable distinct oligomeric intermediates in the presence of heme are roughly 40, 60, 80,

DOI: 10.1021/acs.biochem.5b00280
Biochemistry 2015, 54, 4599−4610

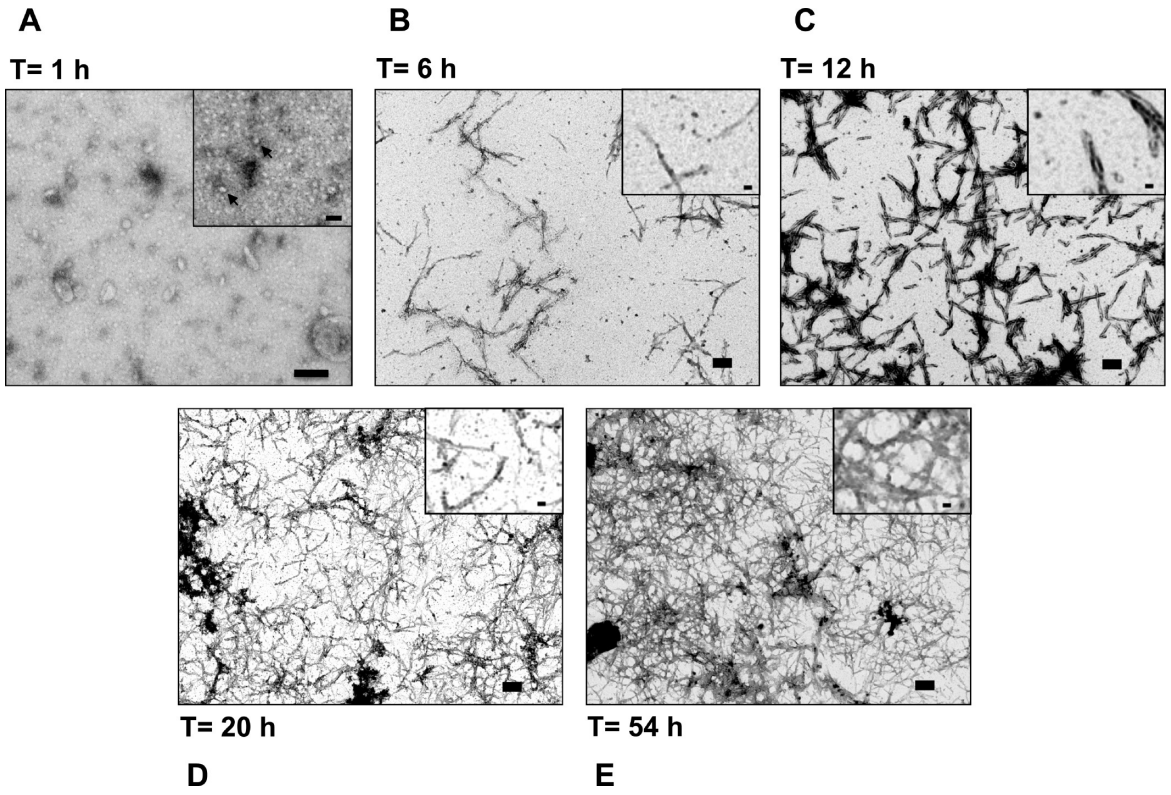

Figure 4. Transmission electron micrograph of negatively stained αSyn at various stages of incubation. (A) Small spherical oligomers of 10−15 nm are observed to be the primary species at 1 h. The scale bar is 100 nm. Arrows indicate individual oligomers. The inset scale bar is 30 nm. Times of (B) 6, (C) 12, (D) 20, and (E) 54 h. Small spherical oligomers are observed during the initial stages of aggregation. Primarily fibrils exist after 30 h. The large scale bar is 200 nm; the inset scale bar is 30 nm.

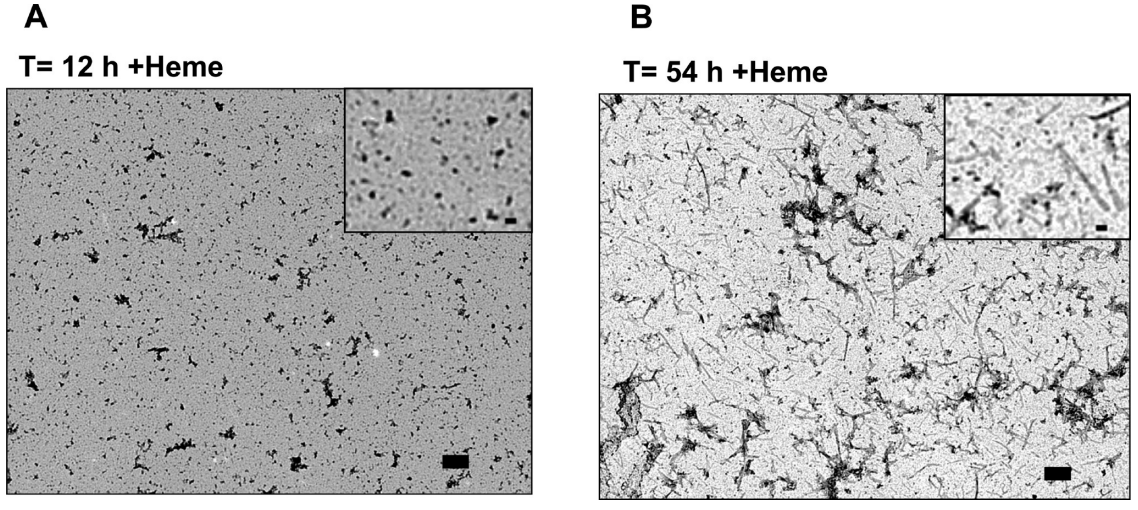

Figure 5. Transmission electron micrographs of negatively stained αSyn in the presence of heme after (A) 12 and (B) 54 h. Small spherical oligomers, which are ≈15 nm in width, are observed throughout the aggregation time course, before the formation of fibrillar structures. The large scale bar is 200 nm; the inset scale bar is 30 nm.

125, 170, and 220 kDa, in addition to protofibrillar and fibrillar structures that eventually formed. These sizes suggest a range of oligomers varying in size from a few to several monomeric units. We hypothesize that the disperse bands in the range below 60 kDa may represent heme-bound species, with an altered migration caused by the charged heme. Interestingly, we observe the disappearance of the upper band of the 60 kDa doublet after the 28 h time point, and the eventual decrease in intensity of the lower band, although it persists through 136 h. The overall intensity of the remaining lanes appears to be less intense after the 28 h lane, presumably because of blotting defects, aggregates that adhere to the sample tube, or chemiluminescent detection artifacts.

The large differences observed between the stable species populated with heme and those without heme could result from a kinetic difference in which similar oligomeric states are transiently populated during the early steps of aggregation without heme. To address this possibility, the aggregation of

DOI: 10.1021/acs.biochem.5b00280
Biochemistry 2015, 54, 4599−4610

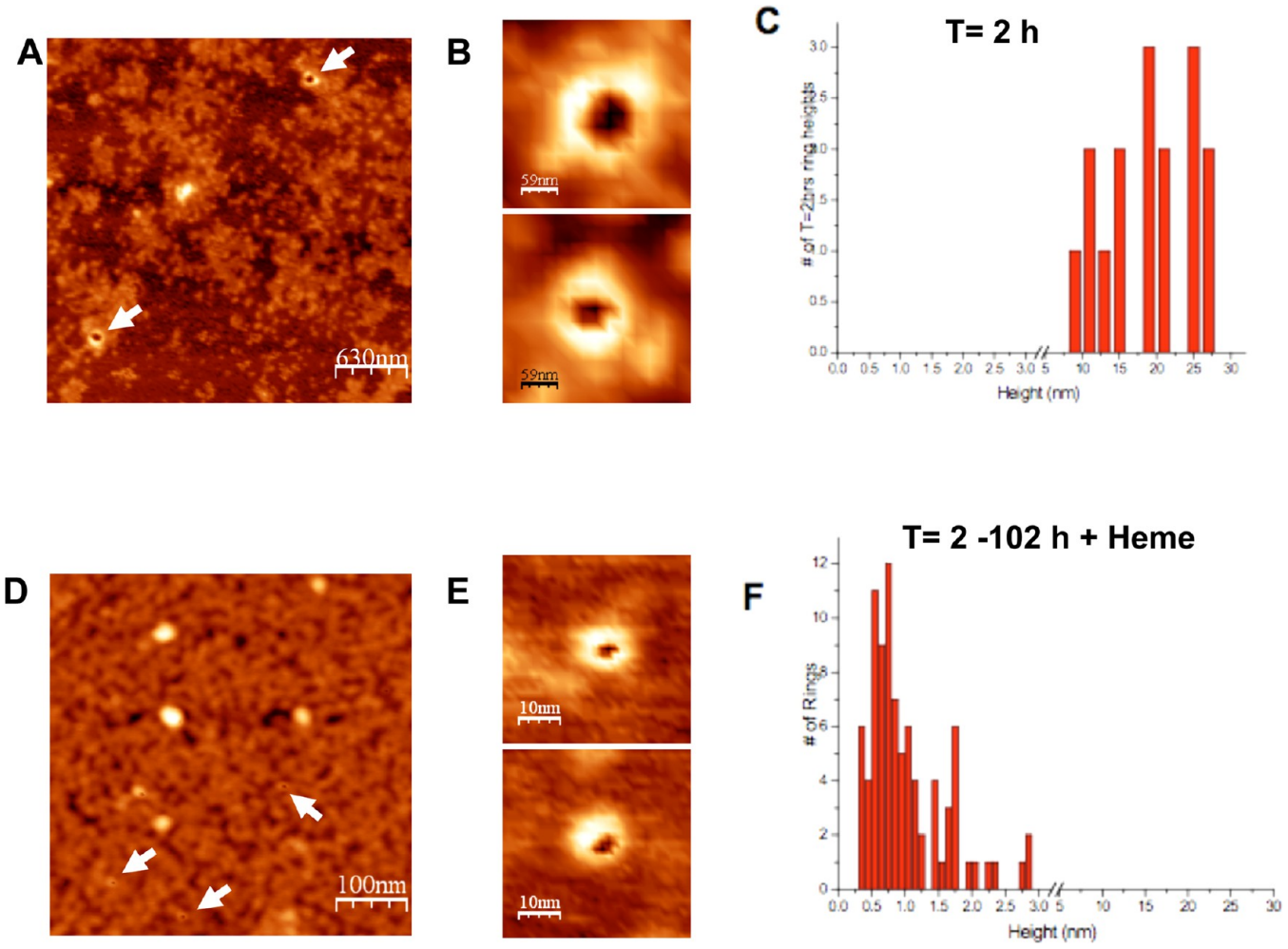

Figure 6. Atomic force microscopy of αSyn aggregates. (A) Two hour incubation of αSyn showing prefibrillar oligomeric structures and annular protofibrils (arrowheads). (B) Typical annular structures. Note the scale bar is 59 nm. (C) Histogram displaying the average height of 18 nm for annular structures formed after aggregation for 2 h (n = 16). (D) Two hour incubation of αSyn in the presence of heme, showing prefibrillar oligomeric structures and annular protofibrils (arrowheads). (E) Typical annular structures. Note the scale bar is 10 nm. (F) Histogram of the heights of annular structures formed in the presence of heme throughout the aggregation time course, showing an average height of 0.9 nm (n = 87).

αSyn after <4 h, in the absence of heme, was examined by native PAGE (Figure 2B). The samples were taken at 15 or 30 min intervals between 0 and 4 h. The predominant doublet at 60 kDa was detected at each time point through 4 h of aggregation in the absence of any higher oligomeric state of αSyn. We observed a band at 40 kDa present throughout the 4 h aggregation, which can also be seen in Figure 2 in the presence of heme. On the basis of these data, we conclude that the ladder of increasing larger oligomeric species is not populated in the absence of heme or, alternately, not stabilized long enough to be detected.

Transmission Electron Microscopy Determination of the Structure of αSyn Aggregates. Negative stain TEM was performed to determine the morphology of the aggregates. After aggregation for 1 h in the absence of heme, the primary species observed were 10−20 nm diameter spherical oligomeric aggregates along with some larger structures ranging in size from 30 to 80 nm (Figure 4A). At incubation times of 6, 12, 20, and 54 h, increasing amounts of typical amyloid fibrils were observed (Figure 4B−E). These amyloid fibril structures of αSyn had lengths of up to 1 μm and were between 15 and 40 nm wide, some with twisted morphology. In contrast, the aggregation process in the presence of heme is very different. Even at after incubation for 12 h, no fibril structures are observed. Instead, as shown in Figure 5A, the sample is composed of small nonfibrillar structures of varying sizes ranging from 10 to 30 nm, likely corresponding to oligomeric structures, consistent with the presence of a ladder of oligomeric structures in the native PAGE experiments. At 54 h (Figure 5B), round oligomeric morphologies are observed in addition to fibrils. These data are representative of two different experiments and indicate that the presence of heme slows and inhibits αSyn fibril formation and concomitantly stabilizes prefibrillar oligomeric intermediates.

Atomic Force Microscopy of Prefibrillar αSyn Intermediates Reveals Annular Structures. To further characterize the structures observed from TEM and native PAGE experiments, structural analysis using atomic force microscopy (AFM) was performed. Aliquots from incubating samples were removed at the indicated times and then adsorbed onto freshly cleaved mica. As shown in Figure 6A, after incubation for 2 h, the samples are comprised of prefibrillar oligomeric structures and a small population of annular protofibrils (arrows), with typical annular structures displaying a central pore. Two examples of annuli are shown enlarged in Figure 6B. The dimensions of the annular structures were individually analyzed

DOI: 10.1021/acs.biochem.5b00280
Biochemistry 2015, 54, 4599−4610

using the WSxM software.[26] The average height of the annular structures was 18 nm, based on images from multiple areas of the 2 h sample. The height ranged from 10 to 25 nm. A histogram of the individual annular heights is shown in Figure 6C (n = 16). Because of sample-tip convolution during AFM, lateral distances cannot be measured as accurately as heights;[34] however, the apparent diameter is on the order of 60 nm. The ability of the AFM tip to resolve a distinct central porelike feature may depend on experimental conditions such as tip morphology or tip contamination from sample. At later aggregation times, a large number of typical amyloid fibrils are present, but there are no observable annular structures (data not shown).

In comparison, a 2 h incubation with heme results in the formation of annular structures and amorphous structures (Figure 6D). Two examples of annular structures are shown in Figure 6E. In the presence of heme, annular structures are observed over the entire time scale (102 h). A histogram of the heights of annular structures thus includes annular structures from 2 to 102 h. The average height of these structures was measured and calculated to be 0.9 nm, ranging from 0.5 to 3 nm, with an apparent diameter of 10 nm [Figure 6F (n = 87)]. The difference in height between annular structures formed without heme and with heme is a factor of nearly 20 (0.9 nm with heme and 18 nm without), while the apparent diameter is approximately 6 times smaller (10 nm with heme and 60 nm without).

Heme Alters the Progression of Secondary Structure Changes during Aggregation. To determine the secondary structures formed prior to amyloid fibril formation, we measured the circular dichroism (CD) spectrum of αSyn in the absence and presence of heme during the aggregation time course. CD spectroscopy is a valuable tool for characterizing the secondary structures present, although large amyloid fibrils are likely to scatter light rather than contribute to the spectral signal.[35] At the start of the time course in the absence of heme, the CD spectrum of αSyn displayed the expected shape for unstructured or random coil protein with a minimum of ellipticity at 202 nm (Figure 7A). Between 0 and 8 h, there was a gradual increase in the ellipticity at this wavelength, with the concomitant development of a minimum at ∼222 nm, suggesting that there may be some contribution of α-helical content prior to the formation of the predominant β-sheet structures. This observation is consistent with a mechanism whereby prefibrillar structures of many types form prior to the rearrangement into classical amyloid antiparallel β-sheet conformations.[36,37] By 28 h, the ellipticity below 200 nm became positive and the feature at 222 nm shifted to 218 nm, corresponding to an increasing contribution from β-sheet secondary structures. From 52 to 136 h, the secondary structure indicated by the CD spectrum showed little change. These spectra had a minimum at 218 nm, a shoulder close to 210 nm, and a positive peak below 200 nm. This overall shape is consistent with a dominant β-sheet secondary structure, with a minor contribution of α-helical content.

In comparison, in the presence of heme, we observed the expected shape for an unstructured or random coil protein with a minimum at 202 nm (Figure 7B) This spectral shape remained nearly unchanged, except for a minor increase in ellipticity of the 202 nm feature, during the 8 h aggregation. By 28 h, the intensity below 200 nm increased to zero, while a double minimum in ellipticity at 210 and 220 nm appeared. This overall spectral shape, which was stable until the end of the time course (136 h), is consistent with a dominant α-helical secondary structure, with a minor β-sheet contribution. Thus, in the presence of heme, αSyn remained unstructured for a longer period of time and displayed more α-helical content and less β-sheet by 136 h in comparison to those of αSyn without heme.

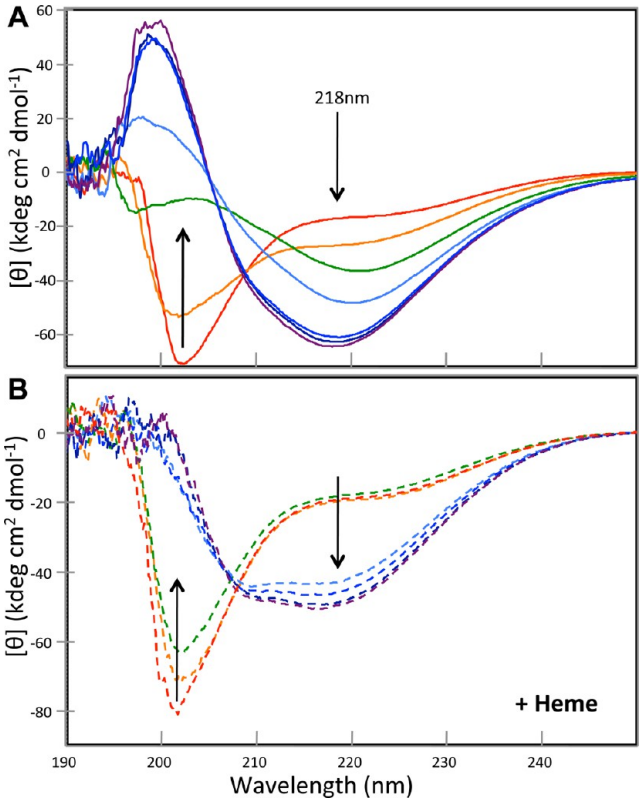

Figure 7. Circular dichroism spectra showing the secondary structure changes of αSyn during the time course of aggregation. (A) Spectral changes at 0, 4, 8, 28, 52, 100, and 136 h, displaying a transition from unstructured to primarily β-sheet structure with a minimum at 218 nm. (B) Spectral changes of αSyn in the presence of heme, at the identical time points as in panel A, showing a secondary structure transition from unstructured to a partially structured combination of α-helical and β-sheet structure at the end of the aggregation time course.

To approximate the secondary structure composition of each CD spectra, we conducted component analysis using CDPro[38] (Figure S1 of the Supporting Information). We used the CONTIN/LL and CONTIN3 basis spectra, from ref 27. While the values for α-helical, β-sheet, and statistical coil structure may not be accurate in the absolute sense, one can see that the relative content of these forms of secondary structure is consistent with that observed above. In particular, in the presence of heme, more unordered structure, 37% at 136 h, remains as compared to 32% without heme. The most striking difference is that the dominant secondary structure remains "unordered" at all aggregation times in the presence of heme, whereas αSyn converts to β-sheet as the predominant structure after 52 h.

Permeation of Large Unilamellar Vesicles. On the basis of the structural differences of the oligomers formed by αSyn compared to the smaller structures we observed in the presence of heme, and the potential physiological implications of these findings, we sought to determine if there were differences in the ability of these structures to disrupt the membrane of vesicles.

DOI: 10.1021/acs.biochem.5b00280
Biochemistry 2015, 54, 4599−4610

Table 1. Comparison of αSyn Structures Observed by ThT Fluorescence, Native PAGE, TEM, AFM, and CD Spectroscopy in the Presence and Absence of Heme

technique	αSyn	αSyn with heme	comments
ThT fluorescence	4 h, lag phase	15 h, lag phase	heme extends lag phase and has a reduced level of aggregate formation
	4−120 h, strong fluorescence	15−120 h, weak fluorescence	
native PAGE	0 h, doublet near 60 kDa	0 h, doublet near 60 kDa	heme results in the formation of stable low-molecular weight oligomers, which have long time stability
	4 h, aggregation, no defined oligomers	2 h, stable oligomer (80 kDa) detected	
	136 h, high-MW component of doublet disappears	4−100 h, multiple oligomers detected	
		28 h, high-MW component of doublet disappears	
TEM	1 h, 10−80 nm structures detected	12 h, 10−30 nonfibrillar structures detected, no fibrils	heme leads to the formation of stable round oligomer structures
	6−54 h, amyloid fibrils grow in	54 h, round oligomeric structures and fibrils detected	
AFM	2 h, prefibrillar oligomers and annular structures 18 nm in height	2 h, amorphous structures and annular structures 0.9 nm in height	annular structures are formed in the presence and absence of heme, but they have very different sizes
	90 h, amyloid fibrils and no annular structures	102 h, annular structures observed at all times measured	
CD	0 h, random coil	0 h, random coil	in the absence of heme, β-sheet structure develops, but in the presence of heme, α-helical structure is formed
	0−8 h, α-helical development	0−8 h, no changes	
	28 h, conversion to β-sheet	28 h, α-helix emerges	

To do so, we prepared calcein-containing large unilamellar vesicles (LUVs) 100 nm in diameter, comprised of 1,2-dioleoyl-*sn*-glycero-3-phospho(1′-*rac*-glycerol) (DOPG), using a slightly modified previously published protocol.[39] The calcein contained inside the vesicle self-quenches and, when released, by disruption of the membrane containing it, can be detected by fluorescence using an excitation wavelength of 490 nm and an emission wavelength of 520 nm. Ten micromolar αSyn or αSyn with equimolar heme at 24 h was added to the LUVs in a 96-well plate. Triton X-100 was used to determine 100% calcein release, and the results were normalized to this value. After incubation for 2 h, αSyn caused 22% calcein release, while αSyn with heme caused 25% calcein release. Buffer, or heme alone, caused a nearly identical calcein release of 8.5% (Figure S2 of the Supporting Information).

DISCUSSION

The experiments reported here demonstrate that the addition of heme to αSyn stabilizes structures, which we do not observe in the absence of heme, and has a dramatic effect on the oligomerization and/or aggregation as summarized in Table 1. Specifically, the presence of heme extends the lag phase for fibril formation and reduces the total amount of fibril formation by 1 order of magnitude. In addition to the decrease in the level of amyloid fibril formation, in the presence of heme, the morphology of the oligomers of αSyn that are formed is dramatically different, consisting of short nonfibrillar structures. Multimeric prefibrillar structures can be detected only in the presence of heme, demonstrating a greater degree of stability for low-molecular weight oligomeric species. Also noteworthy is the fact that the secondary structure analysis revealed a greater α-helical content of the small oligomers in the presence of heme, in contrast to the dominant β-sheet conformation seen in its absence. In summary, the presence of heme appears to stabilize relatively small oligomeric α-helical structures that do not readily convert to the typical fibrillar structures associated with the pathology of αSyn. It is interesting to consider the unique insight provided by the techniques used herein and piece together the information they provide to develop a complete picture of the system under study. Native PAGE indicated that a series of oligomers of increasing size are present during aggregation with heme; however, by AFM, we observed relatively uniform annular structures. The various oligomers observed by native PAGE could account for the large amount of small amorphous material seen by AFM. Similarly, TEM and AFM suggest annular structures are formed in the absence of heme, which could account for the high-molecular weight material caught at the well bottom as seen by native PAGE.

Many different forms of αSyn oligomers have been reported in the past with vastly different morphologies ranging from small spherical structures to annular structures of varying sizes to long protofibril chains to fibrous tangles,[40] each dependent on the conditions under which the oligomerization studies were conducted as well as the incubation time. Annular structures with diameters of 18−27 nm and a height of 3 nm have been observed upon interaction with vesicles and annular structures ranging in size from 30 to 180 nm in diameter and 3 to 10 nm in height have been observed under a variety of conditions.[6,11,13,40−42] Our observations of large size annular structures (∼18 and ∼60 nm in height and apparent diameter, respectively) in the absence of heme are consistent with prior observations, but the smaller structures in the presence of heme (∼1 and 10 nm in height and apparent diameter, respectively) indicate the strong effect of the heme on the structure. On the other hand, it is noteworthy that the A30P and A53T mutants that are associated with early onset Parkinson's disease also formed small annular structures 10−12 nm in diameter.[43] Annular structures have been examined for their ability to interact with membranes and form channels and, indeed, exhibit ion currents.[11,44]

The size and morphology of the αSyn oligomers have been postulated to be a critical factor in its pathophysiology. An "amyloid pore" hypothesis has been proposed, in which an oligomeric ring structure of an amyloid-forming protein forms a toxic pore by incorporation into neuronal membranes. This mechanism is similar to bacterial pore-forming toxins[45] and allows the flow of molecules or ions across the membrane.[11,46]

DOI: 10.1021/acs.biochem.5b00280
Biochemistry 2015, 54, 4599−4610

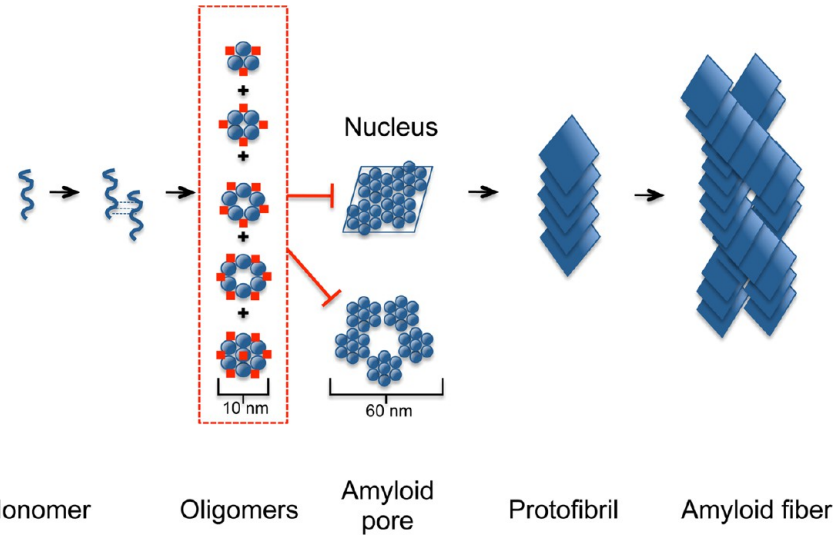

Figure 8. Postulated model for amyloid fibril formation in the presence of heme. Heme (red squares) directly interacts with αSyn-stabilizing oligomeric structures (red box) and inhibits the further aggregation into fibrillar structures. Low-molecular weight oligomers are particularly stabilized by interaction with heme, reducing the chance of formation of nuclei, and shift the equilibrium away from fibril formation. The annular structures stabilized by heme are 10 nm in apparent diameter, whereas the annular structures typically formed are on the order of 60 nm in diameter.

The unregulated movement of ions or other molecules across the neuronal membrane would disrupt their critical levels on both the inside and outside of the cell and in turn trigger neuronal cell death. The formation of pores by Aβ and αSyn was found to be accelerated by mutations associated with familial Alzheimer's and Parkinson's diseases, respectively, suggesting that their formation is related to pathogenic activity.[6] In contrast, recent work attempting to understand the mechanism of toxicity of the αSyn pore came to the conclusion that leakage effects may in fact be caused by bilayer defects due to membrane instability, and not a pore-type mechanism.[47] Our data show that structures formed after 24 h by αSyn or αSyn with heme each disrupt vesicles to a similar extent, suggesting that the size of the structure formed may not be the crucial factor in membrane disruption. There are a number of reasons only a slight difference in ability to disrupt the vesicle membrane between αSyn structures with and without heme was observed. First, the membrane composition may not serve as a fair representation of the physiological membrane, or even a membrane favorable for αSyn interactions. Others have shown αSyn interacts with POPC/POPA or DOPC/DOPS/DOPE small unilamellar vesicles.[23] The size of the vesicles used in our study may also have been a factor. Further, the ability of αSyn structures to interact with a membrane surface may depend on structure formation in the presence of that membrane, and structures formed *in vitro* and added later may behave differently.

On the basis of the new evidence reported here, we propose a model (Figure 8) for the altered aggregation structure and dynamics of αSyn induced by the presence of heme. In this model, the low-molecular weight oligomers are stabilized by interaction with heme, and the formation of larger fibril nuclei that lead to protofibril formation is effectively blocked. Consequently, the formation of the large amyloid fibril aggregates is inhibited or at least greatly retarded. Although we observed a similar level of membrane disruption for the structures formed in the absence or presence of heme, the structures may behave differently *in vivo*.

This model is strongly supported by our AFM data, which reveal that in the presence of heme, annular structures of αSyn were preferentially formed, showing that the presence of heme diverts the aggregation to form oligomeric structures (annular and amorphous), and not fibrils. Moreover, the annular structures stabilized by heme are significantly smaller in width and height (≈10 and 1 nm, respectively) than the annular structures formed in the absence of heme (≈60 and 18 nm, respectively). Annular structures were infrequent in the absence of heme, observed only at 2 h, and were not observed by AFM past 2 h, likely because of their low relative abundance in the sample, or differential adsorption onto the mica surface. Furthermore, consistent with native PAGE data showing oligomers throughout the time course in the presence of heme, AFM data also confirm the presence of annular structures through the longest time point measured, 102 h. We found that their size is constant, as shown by analysis of 87 individual annular structures in Figure 6F.

Using a sphere as a model for a monomeric unit, one can arrange five units into a "pentamer" of roughly pentagonal shape, or six units into a "hexamer" of roughly hexagonal shape. With these shape scaffolds, we can estimate that a monomer with a postulated size of ∼3.3 nm would form a pentamer configuation with an outer diameter of ∼8 nm and an inner diameter of ∼1 nm, whereas a hexamer configuration would have an outer diameter of ∼10 nm and an inner diameter of ∼1.5 nm. On the basis of the annular structures' size as measured by AFM, the structures may be composed of six monomeric subunits. These postulated structures are consistent with molecular modeling studies by Masliah and co-workers, who reported that pentameric and hexameric conformations of the αSyn multimers could form on the membrane.[13,48]

In addition to the effect of heme on αSyn, the pathophysiology of AD may also be affected by the interaction of heme (Fe^{2+}) and/or hemin (Fe^{3+}) with the amyloid β-protein (Aβ).[29,49,50] After incubation with heme, monomers and small Aβ aggregates (e.g., tetramers and trimers) were stabilized according to SDS−PAGE, whereas in the absence of heme, only high-molecular weight Aβ aggregates were

DOI: 10.1021/acs.biochem.5b00280
Biochemistry 2015, 54, 4599−4610

detected.[50] Furthermore, the binding of Aβ to heme is believed to cause heme deficiency in cells, resulting in many of the key cytopathologic characteristics of AD, including selective loss of mitochondrial complex IV, mitochondrial dysfunction, loss of iron homeostasis, and increased production of hydrogen peroxide.[51,52] It has been observed that the Aβ−heme complex exhibits peroxidase activity, potentially catalyzing the oxidation and depletion of various neurotransmitters.[50]

The impact of the interaction of αSyn with heme described in this work opens exciting prospects for future experiments. Indeed, there is great interest in inhibitors of amyloid toxicity. Previous reports have examined small molecule inhibitors and also found inhibition of fibril formation, stabilization of oligomers, and reduction in toxicity (baicalein,[53] EGCG,[33] and gallic acid[54]). Our study, combined with the results of previous work, suggests that heme may be able to slow fibril formation and dismantle amyloid aggregates.[21,50,55] If, in fact, *in vivo* annular structures are cytotoxic, the ability of heme to stabilize different annular structures that are much smaller could prove to be beneficial for PD and other neurodegenerative diseases.

CONCLUSIONS

The data reported here demonstrate that heme can alter the progression of αSyn aggregation, apparently by stabilizing distinct small oligomeric conformations, thereby inhibiting the aggregation process. The presence of heme promotes the formation of annular structures, similar to those that are formed most rapidly by pathogenic mutations of αSyn.[6] As heme is available under physiological conditions with cellular levels of approximately 100 nM,[56] the possibility exists that it could interact with αSyn. However, whether the small oligomeric structures and the annular structures formed in the presence of heme also form *in vivo* and are cytotoxic or whether retardation of the formation of larger oligomeric species is protective against PD remains to be determined.

ASSOCIATED CONTENT

Supporting Information

Supplemental methods describing the calcein release assay, CD component analysis (Figure S1), and calcein release data (Figure S2). The Supporting Information is available free of charge on the ACS Publications website at DOI: 10.1021/acs.biochem.5b00280.

AUTHOR INFORMATION

Corresponding Authors

*E-mail: ehayden@ucla.edu. Phone: (310) 206-2300. Fax: (310) 206-1700.

*E-mail: denis.rousseau@einstein.yu.edu. Phone: (718) 430-4264. Fax: (718) 430-8808.

Present Address

[‖]E.Y.H.: Department of Neurology, David Geffen School of Medicine, University of California, Los Angeles, Los Angeles, CA 90095.

Author Contributions

E.Y.H. performed the experiments. P.K. and E.Y.H. performed the AFM measurements. H.M. provided guidance on AFM. T.L.W. performed the calcein release assay. E.Y.H., S.-R.Y., and D.L.R. planned the experiments and wrote the manuscript.

Funding

Atomic force microscopy and data analysis were supported by Grant MD007599 from the National Institute on Minority Health and Health Disparities (NIMHD) of the National Institutes of Health (NIH). This work was supported by NIH Grant 5T32GM008572, the Molecular Biophysics training grant at the Albert Einstein College of Medicine, NIH Grant GM098799 to D.L.R., and NIH Grant GM086482 to S.-R.Y.

Notes

The authors declare no competing financial interest.

ACKNOWLEDGMENTS

We thank the Analytical Imaging Facility at the Albert Einstein College of Medicine for their assistance with electron microscopy, Dr. Ed Manning and Dr. Nurxat Nuraje for their assistance with AFM measurements, and Dr. David B. Teplow and Dr. Gal Bitan for helpful discussions.

ABBREVIATIONS

PD, Parkinson's disease; AD, Alzheimer's disease; αSyn, α-synuclein; Aβ, amyloid β; ThT, thioflavin T; AFM, atomic force microscopy; TEM, transmission electron microscopy; CD, circular dichroism; LUV, large unilamellar vesicle; DOPG, 1,2-dioleoyl-*sn*-glycero-3-phospho(1′-*rac*-glycerol).

REFERENCES

(1) Glenner, G. G. (1980) Amyloid deposits and amyloidosis. The β-fibrilloses (first of two parts). *N. Engl. J. Med. 302*, 1283−1292.

(2) Bucciantini, M., Giannoni, E., Chiti, F., Baroni, F., Formigli, L., Zurdo, J., Taddei, N., Ramponi, G., Dobson, C. M., and Stefani, M. (2002) Inherent toxicity of aggregates implies a common mechanism for protein misfolding diseases. *Nature 416*, 507−511.

(3) Goedert, M. (2001) α-synuclein and neurodegenerative diseases. *Nat. Rev. Neurosci. 2*, 492−501.

(4) Giasson, B. I., Duda, J. E., Murray, I. V., Chen, Q., Souza, J. M., Hurtig, H. I., Ischiropoulos, H., Trojanowski, J. Q., and Lee, V. M. (2000) Oxidative damage linked to neurodegeneration by selective α-synuclein nitration in synucleinopathy lesions. *Science 290*, 985−989.

(5) Norris, E. H., Giasson, B. I., Hodara, R., Xu, S., Trojanowski, J. Q., Ischiropoulos, H., and Lee, V. M. (2005) Reversible inhibition of α-synuclein fibrillization by dopaminochrome-mediated conformational alterations. *J. Biol. Chem. 280*, 21212−21219.

(6) Lashuel, H. A., Hartley, D., Petre, B. M., Walz, T., and Lansbury, P. T., Jr. (2002) Neurodegenerative disease: amyloid pores from pathogenic mutations. *Nature 418*, 291.

(7) Avidan-Shpalter, C., and Gazit, E. (2006) The early stages of amyloid formation: Biophysical and structural characterization of human calcitonin pre-fibrillar assemblies. *Amyloid 13*, 216−225.

(8) Srinivasan, R., Marchant, R. E., and Zagorski, M. G. (2004) ABri peptide associated with familial British dementia forms annular and ring-like protofibrillar structures. *Amyloid 11*, 10−13.

(9) Volles, M. J., and Lansbury, P. T., Jr. (2003) Zeroing in on the pathogenic form of α-synuclein and its mechanism of neurotoxicity in Parkinson's disease. *Biochemistry 42*, 7871−7878.

(10) Anguiano, M., Nowak, R. J., and Lansbury, P. T., Jr. (2002) Protofibrillar islet amyloid polypeptide permeabilizes synthetic vesicles by a pore-like mechanism that may be relevant to type II diabetes. *Biochemistry 41*, 11338−11343.

(11) Quist, A., Doudevski, I., Lin, H., Azimova, R., Ng, D., Frangione, B., Kagan, B., Ghiso, J., and Lal, R. (2005) Amyloid ion channels: a common structural link for protein-misfolding disease. *Proc. Natl. Acad. Sci. U. S. A. 102*, 10427−10432.

(12) Volles, M. J., Lee, S. J., Rochet, J. C., Shtilerman, M. D., Ding, T. T., Kessler, J. C., and Lansbury, P. T., Jr. (2001) Vesicle permeabilization by protofibrillar α-synuclein: implications for the

DOI: 10.1021/acs.biochem.5b00280
Biochemistry 2015, 54, 4599−4610

pathogenesis and treatment of Parkinson's disease. *Biochemistry 40*, 7812−7819.
(13) Ding, T. T., Lee, S. J., Rochet, J. C., and Lansbury, P. T., Jr. (2002) Annular α-synuclein protofibrils are produced when spherical protofibrils are incubated in solution or bound to brain-derived membranes. *Biochemistry 41*, 10209−10217.
(14) Bartels, T., Choi, J. G., and Selkoe, D. J. (2011) α-Synuclein occurs physiologically as a helically folded tetramer that resists aggregation. *Nature 477*, 107−110.
(15) Wang, W., Perovic, I., Chittuluru, J., Kaganovich, A., Nguyen, L. T., Liao, J., Auclair, J. R., Johnson, D., Landeru, A., Simorellis, A. K., Ju, S., Cookson, M. R., Asturias, F. J., Agar, J. N., Webb, B. N., Kang, C., Ringe, D., Petsko, G. A., Pochapsky, T. C., and Hoang, Q. Q. (2011) A soluble α-synuclein construct forms a dynamic tetramer. *Proc. Natl. Acad. Sci. U. S. A. 108*, 17797−17802.
(16) Burre, J., Vivona, S., Diao, J., Sharma, M., Brunger, A. T., and Sudhof, T. C. (2013) Properties of native brain α-synuclein. *Nature 498*, E4−E6.
(17) Chandra, S., Chen, X., Rizo, J., Jahn, R., and Sudhof, T. C. (2003) A broken α-helix in folded α-Synuclein. *J. Biol. Chem. 278*, 15313−15318.
(18) Davidson, W. S., Jonas, A., Clayton, D. F., and George, J. M. (1998) Stabilization of α-synuclein secondary structure upon binding to synthetic membranes. *J. Biol. Chem. 273*, 9443−9449.
(19) Perrin, R. J., Woods, W. S., Clayton, D. F., and George, J. M. (2000) Interaction of human α-Synuclein and Parkinson's disease variants with phospholipids. Structural analysis using site-directed mutagenesis. *J. Biol. Chem. 275*, 34393−34398.
(20) Uversky, V. N., and Fink, A. L. (2002) Amino acid determinants of α-synuclein aggregation: putting together pieces of the puzzle. *FEBS Lett. 522*, 9−13.
(21) Masuda, M., Suzuki, N., Taniguchi, S., Oikawa, T., Nonaka, T., Iwatsubo, T., Hisanaga, S., Goedert, M., and Hasegawa, M. (2006) Small molecule inhibitors of α-synuclein filament assembly. *Biochemistry 45*, 6085−6094.
(22) Taniguchi, S., Suzuki, N., Masuda, M., Hisanaga, S., Iwatsubo, T., Goedert, M., and Hasegawa, M. (2005) Inhibition of heparin-induced tau filament formation by phenothiazines, polyphenols, and porphyrins. *J. Biol. Chem. 280*, 7614−7623.
(23) Fonseca-Ornelas, L., Eisbach, S. E., Paulat, M., Giller, K., Fernandez, C. O., Outeiro, T. F., Becker, S., and Zweckstetter, M. (2014) Small molecule-mediated stabilization of vesicle-associated helical α-synuclein inhibits pathogenic misfolding and aggregation. *Nat. Commun. 5*, 5857.
(24) Liu, Y., Carver, J. A., Ho, L. H., Elias, A. K., Musgrave, I. F., and Pukala, T. L. (2014) Hemin as a generic and potent protein misfolding inhibitor. *Biochem. Biophys. Res. Commun. 454*, 295−300.
(25) Masuda, M., Dohmae, N., Nonaka, T., Oikawa, T., Hisanaga, S., Goedert, M., and Hasegawa, M. (2006) Cysteine misincorporation in bacterially expressed human α-synuclein. *FEBS Lett. 580*, 1775−1779.
(26) Horcas, I., Fernandez, R., Gomez-Rodriguez, J. M., Colchero, J., Gomez-Herrero, J., and Baro, A. M. (2007) WSXM: a software for scanning probe microscopy and a tool for nanotechnology. *Rev. Sci. Instrum. 78*, 013705.
(27) Provencher, S. W., and Gloeckner, J. (1981) Estimation of globular protein secondary structure from circular dichroism. *Biochemistry 20*, 33−37.
(28) Wood, S. J., Wypych, J., Steavenson, S., Louis, J. C., Citron, M., and Biere, A. L. (1999) α-synuclein fibrillogenesis is nucleation-dependent. Implications for the pathogenesis of Parkinson's disease. *J. Biol. Chem. 274*, 19509−19512.
(29) Atamna, H. (2006) Heme binding to Amyloid-β peptide: Mechanistic role in Alzheimer's disease. *Journal of Alzheimer's disease: JAD 10*, 255−266.
(30) Weinreb, P. H., Zhen, W., Poon, A. W., Conway, K. A., and Lansbury, P. T., Jr. (1996) NACP, a protein implicated in Alzheimer's disease and learning, is natively unfolded. *Biochemistry 35*, 13709−13715.
(31) Guo, A., Han, M., Martinez, T., Ketchem, R. R., Novick, S., Jochheim, C., and Balland, A. (2008) Electrophoretic evidence for the presence of structural isoforms specific for the IgG2 isotype. *Electrophoresis 29*, 2550−2556.
(32) Fauvet, B., Mbefo, M. K., Fares, M. B., Desobry, C., Michael, S., Ardah, M. T., Tsika, E., Coune, P., Prudent, M., Lion, N., Eliezer, D., Moore, D. J., Schneider, B., Aebischer, P., El-Agnaf, O. M., Masliah, E., and Lashuel, H. A. (2012) α-Synuclein in central nervous system and from erythrocytes, mammalian cells, and Escherichia coli exists predominantly as disordered monomer. *J. Biol. Chem. 287*, 15345−15364.
(33) Ehrnhoefer, D. E., Bieschke, J., Boeddrich, A., Herbst, M., Masino, L., Lurz, R., Engemann, S., Pastore, A., and Wanker, E. E. (2008) EGCG redirects amyloidogenic polypeptides into unstructured, off-pathway oligomers. *Nat. Struct. Mol. Biol. 15*, 558−566.
(34) van Raaij, M. E., Segers-Nolten, I. M., and Subramaniam, V. (2006) Quantitative morphological analysis reveals ultrastructural diversity of amyloid fibrils from α-synuclein mutants. *Biophys. J. 91*, L96−98.
(35) Kelly, S. M., Jess, T. J., and Price, N. C. (2005) How to study proteins by circular dichroism. *Biochim. Biophys. Acta, Proteins Proteomics 1751*, 119−139.
(36) Kamiyoshihara, T., Kojima, M., Ueda, K., Tashiro, M., and Shimotakahara, S. (2007) Observation of multiple intermediates in α-synuclein fibril formation by singular value decomposition analysis. *Biochem. Biophys. Res. Commun. 355*, 398−403.
(37) Zakharov, S. D., Hulleman, J. D., Dutseva, E. A., Antonenko, Y. N., Rochet, J. C., and Cramer, W. A. (2007) Helical α-synuclein forms highly conductive ion channels. *Biochemistry 46*, 14369−14379.
(38) Sreerama, N., Venyaminov, S. Y., and Woody, R. W. (2000) Estimation of protein secondary structure from circular dichroism spectra: inclusion of denatured proteins with native proteins in the analysis. *Anal. Biochem. 287*, 243−251.
(39) Williams, T. L., Day, I. J., and Serpell, L. C. (2010) The effect of Alzheimer's Abeta aggregation state on the permeation of biomimetic lipid vesicles. *Langmuir 26*, 17260−17268.
(40) Stockl, M. T., Zijlstra, N., and Subramaniam, V. (2013) α-Synuclein oligomers: an amyloid pore? Insights into mechanisms of α-synuclein oligomer-lipid interactions. *Mol. Neurobiol. 47*, 613−621.
(41) Lowe, R., Pountney, D. L., Jensen, P. H., Gai, W. P., and Voelcker, N. H. (2004) Calcium(II) selectively induces α-synuclein annular oligomers via interaction with the C-terminal domain. *Protein science: a publication of the Protein Society 13*, 3245−3252.
(42) Danzer, K. M., Haasen, D., Karow, A. R., Moussaud, S., Habeck, M., Giese, A., Kretzschmar, H., Hengerer, B., and Kostka, M. (2007) Different species of α-synuclein oligomers induce calcium influx and seeding. *J. Neurosci. 27*, 9220−9232.
(43) Lashuel, H. A., Petre, B. M., Wall, J., Simon, M., Nowak, R. J., Walz, T., and Lansbury, P. T., Jr. (2002) α-synuclein, especially the Parkinson's disease-associated mutants, forms pore-like annular and tubular protofibrils. *J. Mol. Biol. 322*, 1089−1102.
(44) Kayed, R., Pensalfini, A., Margol, L., Sokolov, Y., Sarsoza, F., Head, E., Hall, J., and Glabe, C. (2009) Annular protofibrils are a structurally and functionally distinct type of amyloid oligomer. *J. Biol. Chem. 284*, 4230−4237.
(45) Parker, M. W., and Feil, S. C. (2005) Pore-forming protein toxins: from structure to function. *Prog. Biophys. Mol. Biol. 88*, 91−142.
(46) Kostka, M., Hogen, T., Danzer, K. M., Levin, J., Habeck, M., Wirth, A., Wagner, R., Glabe, C. G., Finger, S., Heinzelmann, U., Garidel, P., Duan, W., Ross, C. A., Kretzschmar, H., and Giese, A. (2008) Single particle characterization of iron-induced pore-forming α-synuclein oligomers. *J. Biol. Chem. 283*, 10992−11003.
(47) van Rooijen, B. D., Claessens, M. M., and Subramaniam, V. (2010) Membrane Permeabilization by Oligomeric α-Synuclein: In Search of the Mechanism. *PLoS One 5*, e14292.
(48) Tsigelny, I. F., Bar-On, P., Sharikov, Y., Crews, L., Hashimoto, M., Miller, M. A., Keller, S. H., Platoshyn, O., Yuan, J. X., and Masliah, E. (2007) Dynamics of α-synuclein aggregation and inhibition of pore-

DOI: 10.1021/acs.biochem.5b00280
Biochemistry 2015, 54, 4599−4610

like oligomer development by beta-synuclein. *FEBS J. 274*, 1862−1877.
(49) Khodarahmi, R., Soori, H., and Karimi, S. A. (2009) Chaperone-like activity of heme group against amyloid-like fibril formation by hen egg ovalbumin: possible mechanism of action. *Int. J. Biol. Macromol. 44*, 98−106.
(50) Atamna, H., and Boyle, K. (2006) Amyloid-β peptide binds with heme to form a peroxidase: relationship to the cytopathologies of Alzheimer's disease. *Proc. Natl. Acad. Sci. U. S. A. 103*, 3381−3386.
(51) Atamna, H., Killilea, D. W., Killilea, A. N., and Ames, B. N. (2002) Heme deficiency may be a factor in the mitochondrial and neuronal decay of aging. *Proc. Natl. Acad. Sci. U. S. A. 99*, 14807−14812.
(52) Atamna, H., Liu, J., and Ames, B. N. (2001) Heme deficiency selectively interrupts assembly of mitochondrial complex IV in human fibroblasts: revelance to aging. *J. Biol. Chem. 276*, 48410−48416.
(53) Zhu, M., Rajamani, S., Kaylor, J., Han, S., Zhou, F., and Fink, A. L. (2004) The flavonoid baicalein inhibits fibrillation of α-synuclein and disaggregates existing fibrils. *J. Biol. Chem. 279*, 26846−26857.
(54) Ardah, M. T., Paleologou, K. E., Lv, G., Abul Khair, S. B., Kazim, A. S., Minhas, S. T., Al-Tel, T. H., Al-Hayani, A. A., Haque, M. E., Eliezer, D., and El-Agnaf, O. M. (2014) Structure activity relationship of phenolic acid inhibitors of α-synuclein fibril formation and toxicity. *Front. Aging Neurosci. 6*, 197.
(55) Gatta, L. B., Vitali, M., Verardi, R., Arosio, P., and Finazzi, D. (2009) Inhibition of heme synthesis alters Amyloid Precursor Protein processing. *J. Neural Transm 116*, 79−88.
(56) Tracz, M. J., Alam, J., and Nath, K. A. (2007) Physiology and pathophysiology of heme: implications for kidney disease. *J. Am. Soc. Nephrol. 18*, 414−420.

DOI: 10.1021/acs.biochem.5b00280
Biochemistry 2015, 54, 4599−4610